Electromagnetic propagation in periodic stratified media. I. General theory*

Pochi Yeh, Amnon Yariv, and Chi-Shain Hong
California Institute of Technology, Pasadena, California 91125
(Received 8 November 1976)

The propagation of electromagnetic radiation in periodically stratified media is considered. Media of finite, semi-infinite, and infinite extent are treated. A diagonalization of the unit cell translation operator is used to obtain exact solutions for the Bloch waves, the dispersion relations, and the band structure of the medium. Some new phenomena with applications to integrated optics and laser technology are presented.

I. INTRODUCTION

Periodic optical media and specifically stratified periodic structures play an important role in a number of applications. These include multilayer high-reflectance coatings for both high reflection and antireflection. This application benefitted largely from the pioneering analysis of Abeles.[1] Other proposals involve the use of these structures for phase matching in nonlinear optical applications[2-4] and for obtaining optical birefringence in stratified media composed of isotropic or cubic materials.[5,6]

Recent developments in the crystal-growing field, especially in molecular beam technology,[7] make is possible to grow multilayer media with well-controlled periodicities and with layer thicknesses down to 10 Å. We may thus well consider the periodic optical structure as a new optical medium to take its place along with that of, say, homogeneous isotropic and anisotropic materials. Before proceeding with the many applications envisaged for periodic media we need to understand precisely and in detail the nature of electromagnetic wave propagation in these media. Although a number of special cases have been analyzed, a general theory is not available. To illustrate this situation we may point out, as one example, that the present state of the theory does not answer questions such as that of the direction of group and energy velocities of waves in periodic media or even that of the birefringence at arbitrary angles of incidence.

The two papers that follow describe a general theory of electromagnetic propagation in periodic media. The theoretical approach is general, so that many situations considered previously will be shown to be special cases of our formalism. The theory has a strong formal similarity to the quantum theory of electrons in crystals and thus makes heavy use of the concepts of Bloch modes, forbidden gaps, evanescent waves, and surface waves.

In addition to demonstrating the application of the theory to a number of familiar problems, such as reflectivity of multilayer films, we consider in general form a variety of some experimental situations which include Bragg waveguides, birefringence and group velocity at arbitrary directions, phase matching in nonlinear optical applications, multichannel waveguides, and optical surface waves. We also consider the important problem of propagation and reflection in media with periodic gain and loss alternation which is relevant to x-ray laser oscillation in artificially layered media.[8]

II. MATRIX METHOD AND TRANSLATION OPERATOR

For the sake of clarity in introducing the basic concepts we will consider first the simplest type of periodically stratified medium. The extension to the more general case is presented in Appendix A. The stratified medium treated in what follows consists of alternating layers of different indices of refraction. The index of refraction profile is given by

$$n(x) = \begin{cases} n_2, & 0<x<b\ , \\ n_1, & b<x<\Lambda\ , \end{cases} \tag{1}$$

with

$$n(x+\Lambda)=n(x)\ , \tag{2}$$

where the x axis is normal to the interfaces and Λ is the period. The geometry of the structure is sketched in Fig. 1. The distribution of some typical field components can be written

$$E(x,z)=E(x)\,e^{i\beta z}\ . \tag{3}$$

The electric field distribution within each homogeneous layer can be expressed as a sum of an incident plane wave and a reflected plane wave. The complex amplitudes of these two waves constitute the components of a column vector. The electric field in the α layer of the nth unit cell can thus be represented by a column vector

$$\begin{pmatrix} a_n^{(\alpha)} \\ b_n^{(\alpha)} \end{pmatrix}\ .$$

As a result, the electric field distribution in the same

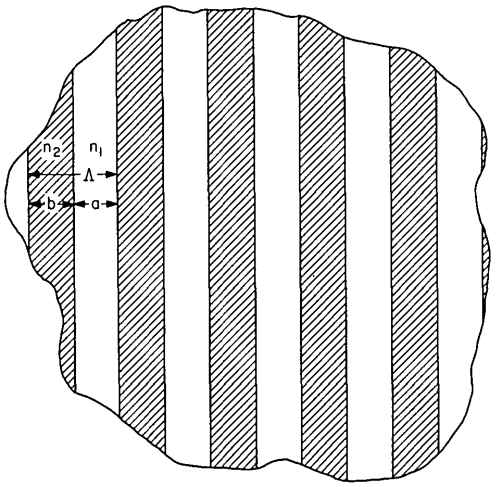

FIG. 1. Portion of a typical periodic stratified medium.

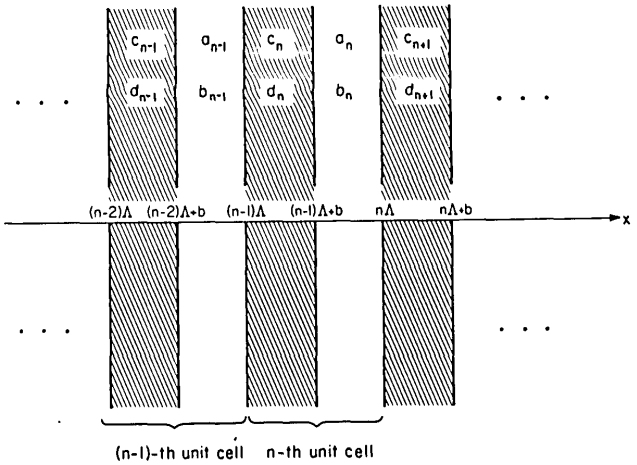

FIG. 2. Plane wave amplitudes associated with the nth unit cell and its neighboring cells.

layer can be written

$$E(x,z) = (a_n^{(\alpha)} e^{ik_{\alpha x}(x-n\Lambda)} + b_n^{(\alpha)} e^{-ik_{\alpha x}(x-n\Lambda)}) e^{i\beta z} , \tag{4}$$

with

$$k_{\alpha x} = \{[(\omega/c)n_\alpha]^2 - \beta^2\}^{1/2}, \quad \alpha = 1, 2 . \tag{5}$$

The column vectors are not independent of each other. They are related through the continuity conditions at the interfaces. As a matter of fact, only one vector (or two components of two different vectors) can be chosen arbitrarily. In the case of TE modes (E vector in y-z plane) imposing continuity of E and $\partial E/\partial x$ at the interface (see Fig. 2) leads to

$$\begin{aligned}
&a_{n-1} + b_{n-1} = e^{-ik_{2x}\Lambda} c_n + e^{ik_{2x}\Lambda} d_n , \\
&ik_{1x}(a_{n-1} - b_{n-1}) = ik_{2x}(e^{-ik_{2x}\Lambda} c_n - e^{ik_{2x}\Lambda} d_n) , \\
&e^{-ik_{2x}a} c_n + e^{ik_{2x}a} d_n = e^{-ik_{1x}a} a_n + e^{ik_{1x}a} b_n , \\
&ik_{2x}(e^{-ik_{2x}a} c_n - e^{ik_{2x}a} d_n) = ik_{1x}(e^{-ik_{1x}a} a_n - e^{ik_{1x}a} b_n) .
\end{aligned} \tag{6}$$

The four equations in (6) can be rewritten as the following two matrix equations:

$$\begin{pmatrix} 1 & 1 \\ 1 & -1 \end{pmatrix} \begin{pmatrix} a_{n-1} \\ b_{n-1} \end{pmatrix}$$

$$= \begin{pmatrix} e^{-ik_{2x}\Lambda} & e^{ik_{2x}\Lambda} \\ \frac{k_{2x}}{k_{1x}} e^{-ik_{2x}\Lambda} & -\frac{k_{2x}}{k_{1x}} e^{ik_{2x}\Lambda} \end{pmatrix} \begin{pmatrix} c_n \\ d_n \end{pmatrix} , \tag{7}$$

$$\begin{pmatrix} e^{-ik_{2x}a} & e^{ik_{2x}a} \\ e^{-ik_{2x}a} & -e^{ik_{2x}a} \end{pmatrix} \begin{pmatrix} c_n \\ d_n \end{pmatrix}$$

$$= \begin{pmatrix} e^{-ik_{1x}a} & e^{ik_{1x}a} \\ \frac{k_{1x}}{k_{2x}} e^{-ik_{1x}a} & -\frac{k_{1x}}{k_{2x}} e^{ik_{1x}a} \end{pmatrix} \begin{pmatrix} a_n \\ b_n \end{pmatrix} , \tag{8}$$

where we define

$$a_n \equiv a_n^{(1)}, \quad b_n \equiv b_n^{(1)} ,$$

$$c_n \equiv a_n^{(2)}, \quad d_n \equiv b_n^{(2)} .$$

By eliminating

$$\begin{pmatrix} c_n \\ d_n \end{pmatrix} ,$$

the matrix equation

$$\begin{pmatrix} a_{n-1} \\ b_{n-1} \end{pmatrix} = \begin{pmatrix} A & B \\ C & D \end{pmatrix} \begin{pmatrix} a_n \\ b_n \end{pmatrix} \tag{9}$$

is obtained. The matrix elements are

$$A = e^{-ik_{1x}a}\left[\cos k_{2x}b - \frac{1}{2}i\left(\frac{k_{2x}}{k_{1x}} + \frac{k_{1x}}{k_{2x}}\right)\sin k_{2x}b\right] , \tag{10}$$

$$B = e^{ik_{1x}a}\left[-\frac{1}{2}i\left(\frac{k_{2x}}{k_{1x}} - \frac{k_{1x}}{k_{2x}}\right)\sin k_{2x}b\right] , \tag{11}$$

$$C = e^{-ik_{1x}a}\left[\frac{1}{2}i\left(\frac{k_{2x}}{k_{1x}} - \frac{k_{1x}}{k_{2x}}\right)\sin k_{2x}b\right] , \tag{12}$$

$$D = e^{ik_{1x}a}\left[\cos k_{2x}b + \frac{1}{2}i\left(\frac{k_{2x}}{k_{1x}} + \frac{k_{1x}}{k_{2x}}\right)\sin k_{2x}b\right] , \tag{13}$$

and according to (5) can be viewed as functions of β. The matrix in (9) is the unit cell translation matrix which relates the complex amplitudes of the incident plane wave a_{n-1} and the reflected plane wave b_{n-1} in one layer of a unit cell to those of the equivalent layer in the next unit cell. Because of the fact that this matrix relates the fields of two equivalent layers with the same index of refraction, it is unimodular, i.e.,

$$AD - BC = 1 . \tag{14}$$

It is important to note that the matrix which relates

$$\begin{pmatrix} c_{n-1} \\ d_{n-1} \end{pmatrix} \text{ to } \begin{pmatrix} c_n \\ d_n \end{pmatrix}$$

is different from the matrix in (9). These matrices, however, possess the same trace (Appendix A). As will be shown later, the trace of the translation matrix is directly related to the band structure of the stratified periodic medium.

The matrix elements (A, B, C, D) for TM waves (H vector in yz vector plane) are slightly different from those of the TE waves. They are given by

$$A_{TM} = e^{-ik_{1x}a}\left[\cos k_{2x}b - \frac{1}{2}i\left(\frac{n_2^2 k_{1x}}{n_1^2 k_{2x}} + \frac{n_1^2 k_{2x}}{n_2^2 k_{1x}}\right)\sin k_{2x}b\right] , \tag{15}$$

$$B_{TM} = e^{ik_{1x}a}\left[-\frac{1}{2}i\left(\frac{n_2^2 k_{1x}}{n_1^2 k_{2x}} - \frac{n_1^2 k_{2x}}{n_2^2 k_{1x}}\right)\sin k_{2x}b\right] , \tag{16}$$

$$C_{TM} = e^{-ik_{1x}a}\left[\frac{1}{2}i\left(\frac{n_2^2 k_{1x}}{n_1^2 k_{2x}} - \frac{n_1^2 k_{2x}}{n_2^2 k_{1x}}\right)\sin k_{2x}b\right] , \tag{17}$$

$$D_{TM} = e^{ik_{1x}a}\left[\cos k_{2x}b + \frac{1}{2}i\left(\frac{n_2^2 k_{1x}}{n_1^2 k_{2x}} + \frac{n_1^2 k_{2x}}{n_2^2 k_{1x}}\right)\sin k_{2x}b\right] . \tag{18}$$

As noted above, only one column vector is independent. We can choose it, as an example, as the column vector of the n_1 layer in the zeroth unit cell. The remaining column vectors of the equivalent layers are given as

$$\begin{pmatrix} a_n \\ b_n \end{pmatrix} = \begin{pmatrix} A & B \\ C & D \end{pmatrix}^{-n} \begin{pmatrix} a_0 \\ b_0 \end{pmatrix} . \tag{19}$$

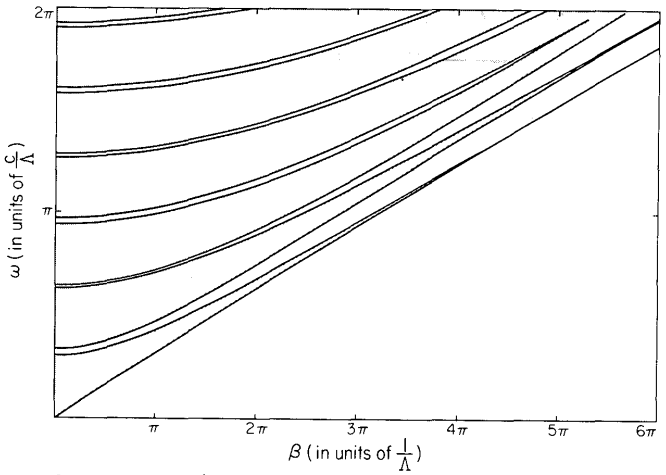

FIG. 3. TE waves (E perpendicular to the direction of periodicity) band structure in the ω-β plane. The dark zones are the allowed bands.

By using (14), the above equation can be simplified to

$$\begin{pmatrix} a_n \\ b_n \end{pmatrix} = \begin{pmatrix} D & -B \\ -C & A \end{pmatrix}^n \begin{pmatrix} a_0 \\ b_0 \end{pmatrix} . \tag{20}$$

The column vector for the n_2 layer can always be obtained by using Eq. (8); more generally, we can specify the field uniquely by specifying any a_i and b_j.

III. BLOCH WAVES AND BAND STRUCTURES

The periodically stratified medium is equivalent to a one-dimensional lattice which is invariant under the lattice translation. The lattice translation operator T is defined by $Tx = x + l\Lambda$, where l is an integer; it follows that

$$TE(x) = E(T^{-1}x) = E(x - l\Lambda) . \tag{21}$$

The $ABCD$ matrix derived in Sec. II is a representation of the unit cell translation operator. According to the Floquet theorem, a wave propagating in a periodic medium is of the form[9]

$$E_K(x, z) = E_K(x)\, e^{iKx} e^{i\beta z} ,$$

where $E_K(x)$ is periodic with a period, Λ, i.e.,

$$E_K(x + \Lambda) = E_K(x) . \tag{22}$$

The subscript K indicates that the function $E_K(x)$ depends on K. The constant K is known as the Bloch wave number. The problem at hand is thus that of determining K and $E_K(x)$.

In terms of our column vector representation, and from (4), the periodic condition (22) for the Bloch wave is simply

$$\begin{pmatrix} a_n \\ b_n \end{pmatrix} = e^{iK\Lambda} \begin{pmatrix} a_{n-1} \\ b_{n-1} \end{pmatrix} . \tag{23}$$

It follows from (9) and (23) that the column vector of the Bloch wave satisfies the following eigenvalue problem:

$$\begin{pmatrix} A & B \\ C & D \end{pmatrix} \begin{pmatrix} a_n \\ b_n \end{pmatrix} = e^{-iK\Lambda} \begin{pmatrix} a_n \\ b_n \end{pmatrix} . \tag{24}$$

The phase factor $e^{-iK\Lambda}$ is thus the eigenvalue of the translation matrix (A, B, C, D) and is given by

$$e^{-iK\Lambda} = \tfrac{1}{2}(A + D) \pm \{[\tfrac{1}{2}(A + D)]^2 - 1\}^{1/2} . \tag{25}$$

The eigenvectors corresponding to the eigenvalues (25) are obtained from (24) and are

$$\begin{pmatrix} a_0 \\ b_0 \end{pmatrix} = \begin{pmatrix} B \\ e^{-iK\Lambda} - A \end{pmatrix} \tag{26}$$

times any arbitrary constant. The Bloch waves which result from (26) can be considered as the eigenvectors of the translation matrix with eigenvalues $e^{\pm iK\Lambda}$ given by (25). The two eigenvalues in (25) are the inverse of each other, since the translation matrix is unimodular. Equation (25) gives the dispersion relation between ω, β, and K for the Bloch wave function

$$K(\beta, \omega) = (1/\Lambda) \cos^{-1}[\tfrac{1}{2}(A + D)] . \tag{27}$$

Regimes where $|\frac{1}{2}(A + D)| < 1$ correspond to real K and thus to propagating Bloch waves, when $|\frac{1}{2}(A + D)| > 1$, $K = m\pi/\Lambda + iK_i$ and has an imaginary part K_i so that the Bloch wave is evanescent. These are the so-called "forbidden" bands of the periodic medium. The band edges are the regimes where $|\frac{1}{2}(A + D)| = 1$.

According to (4) and (23) the final result for the Bloch wave in the n_1 layer of the nth unit cell is

$$E_K(x) e^{iKx} = [(a_0 e^{ik_{1x}(x - n\Lambda)} + b_0 e^{-ik_{1x}(x - n\Lambda)})\, e^{-iK(x - n\Lambda)}]\, e^{iKx} , \tag{28}$$

where a_0 and b_0 are given by Eq. (26). This completes the solution of the Bloch waves.

The band structure for a typical stratified periodic medium as obtained from (27) is shown in Figs. 3 and 4 for TE and TM waves, respectively. It is interesting to notice that the TM "forbidden" bands shrink to zero when $\beta = (\omega/c) n_2 \sin\theta_B$ with θ_B as the Brewster angle, since at this angle the incident and reflected waves are

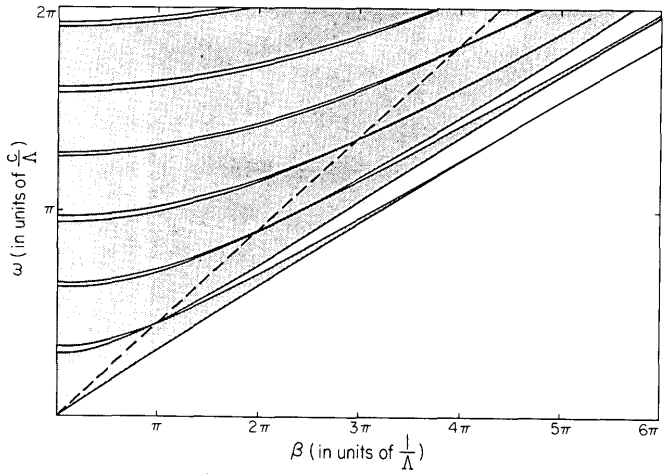

FIG. 4. TM waves (H perpendicular to the direction of periodicity) band structure in the ω-β plane. The dashed line is $\beta = (\omega/c) n_2 \sin\phi_B$. The dark zones are the allowed bands.

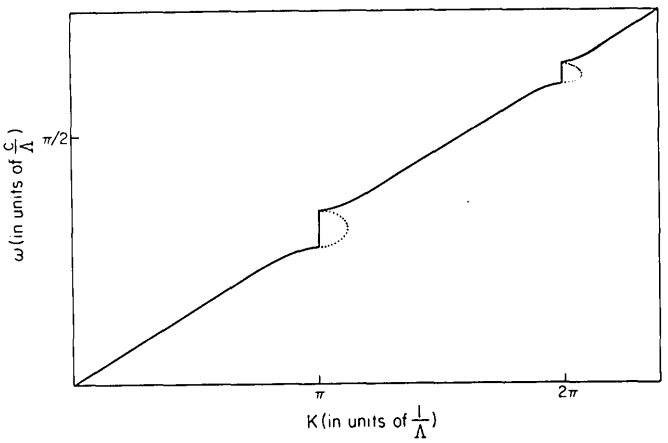

FIG. 5. Dispersion relation between ω and K when $\beta = 0$ (normal incidence). Dotted curves are the imaginary part of K in arbitrary scales.

uncoupled. The dispersion relation ω vs K for the special case $\beta = 0$, i.e., normal incidence, is shown in Fig. 5.

IV. BRAGG REFLECTOR

Periodic perturbation in a dielectric medium has been used extensively in fabricating distributed feedback lasers[10,11] (DFB) and distributed Bragg reflection lasers[12] (DBR). Corrugation over the guiding layer is the usual way of providing periodic perturbation. The optical fields are determined by using the coupled-mode theory[13] which in a truncated (finite number of terms) form is a very good approximation as long as the perturbation is small. In the case of square well alternation which corresponds to the layered medium described above, an exact solution is obtained by our matrix method.

Consider a periodically stratified medium with N unit cells. The geometry of the structure is sketched in Fig. 6. The coefficient of reflection is given by

$$r_N = (b_0/a_0)_{b_N=0} . \tag{29}$$

From (19) we have the following relation:

$$\begin{pmatrix} a_0 \\ b_0 \end{pmatrix} = \begin{pmatrix} A & B \\ C & D \end{pmatrix}^N \begin{pmatrix} a_N \\ b_N \end{pmatrix} . \tag{30}$$

The Nth power of an unimodular matrix can be simplified by the following matrix identity[14] (see Appendix B):

$$\begin{pmatrix} A & B \\ C & D \end{pmatrix}^N = \begin{pmatrix} AU_{N-1} - U_{N-2} & BU_{N-1} \\ CU_{N-1} & DU_{N-1} - U_{N-2} \end{pmatrix} , \tag{31}$$

where

$$U_N = \sin(N+1)K\Lambda / \sin K\Lambda , \tag{32}$$

with K given by Eq. (27).

The coefficient of reflection is immediately obtained from (29), (30), and (31) as

$$r_N = CU_{N-1}/(AU_{N-1} - U_{N-2}) . \tag{33}$$

The reflectivity is obtained by taking the absolute square of r_N,

$$|r_N|^2 = \frac{|C|^2}{|C|^2 + (\sin K\Lambda / \sin NK\Lambda)^2} . \tag{34}$$

We have in (34), the first published analytic expression of the reflectivity of a multilayer reflector. The term $|C|^2$ is directly related to the reflectivity of a single unit cell by

$$|r_1|^2 = |C|^2/(|C|^2 + 1) \tag{35}$$

or

$$|C|^2 = |r_1|^2/(1 - |r_1|^2) . \tag{36}$$

The $|r_1|^2$ for a typical Bragg reflector is usually much less than one. As a result, $|C|^2$ is roughly equal to $|r_1|^2$. The second term in the denominator of (34) is a fast varying function of K, or alternatively, of β and ω. Therefore, it dominates the structure of the reflectivity spectrum. Between any two "forbidden" bands there are exactly $N-1$ nodes where the reflectivity vanishes. The peaks of the reflectivity occur at the centers of the "forbidden" bands. There are exactly $N-2$ side lobes which are all under the envelope $|C|^2/[|C|^2 + (\sin K\Lambda)^2]$. At the band edges, $K\Lambda = m\pi$ and the reflectivity is given by

$$|r_N|^2 = |C|^2/[|C|^2 + (1/N)^2] . \tag{37}$$

In the "forbidden" gap $K\Lambda$ is a complex number

$$K\Lambda = m\pi + iK_i\Lambda . \tag{38}$$

The reflectivity formula of (34) becomes

$$|r_N|^2 = \frac{|C|^2}{|C|^2 + (\sinh K_i\Lambda / \sinh NK_i\Lambda)^2} . \tag{39}$$

For large N the second term in the denominator approaches zero exponentially as $e^{-2(N-1)K_i\Lambda}$. It follows that the reflectivity in the forbidden gap is near unity for a Bragg reflector with a substantial number of periods.

TE and TM waves have different band structures and different reflectivities. For TM waves incident at the Brewster angle there is no reflected wave. This is due to the vanishing of the dynamical factor $|C|^2$

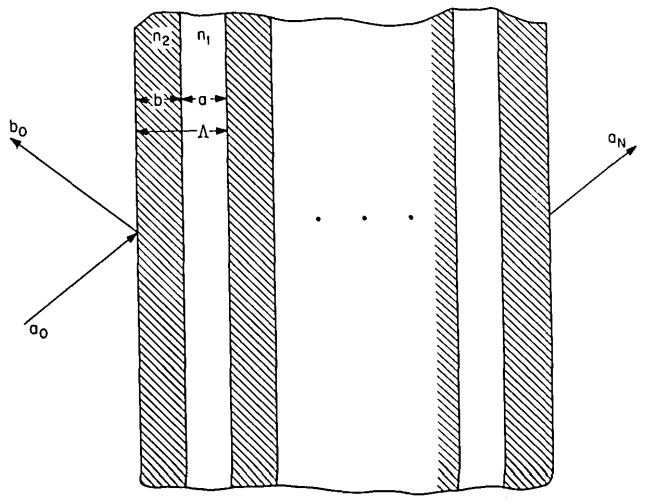

FIG. 6. Geometry of a typical N-period Bragg reflector.

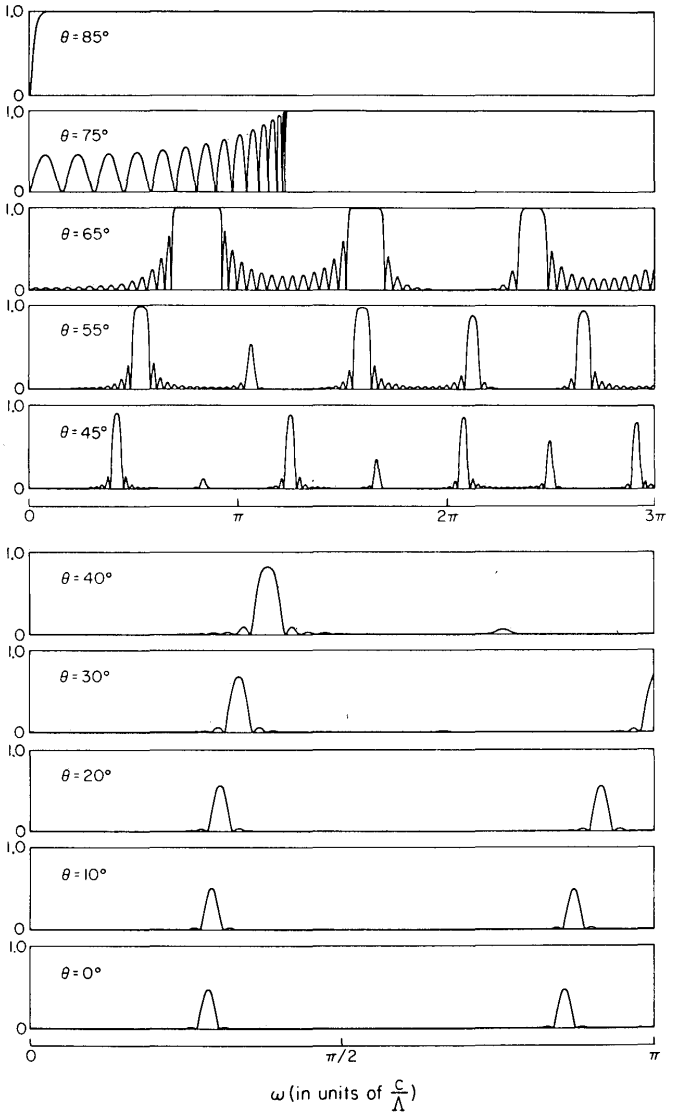

FIG. 7. TE waves reflectivity spectrum of a 15-period Bragg reflector at various angles of incidence.

at that angle.

The reflectivity for some typical Bragg reflectors as a function of frequency and angle of incidence are shown in Figs. 7 and 8.

V. GUIDED WAVES

Multilayer waveguides are becoming increasingly important in integrated optics. The two-channel dielectric waveguides have been studied extensively in the theory of branching waveguides[15,16] which is used in fabricating mode selectors, switches, and directional couplers in integrated optics.[17] The analytic treatment for the general N-channel waveguide, however, suffers from the serious difficulty of solving an eigenvalue problem involving a $4N \times 4N$ matrix, and has relied heavily on numerical techniques.

In the present analysis we employ the matrix method described in Sec. II that involves only the manipulation of 2×2 matrices. Of particular interest is the periodic multichannel dielectric waveguide (PMDW) which consists of a stack of dielectric layers of alternating indices of refraction. Analytic expressions for the mode dispersion relations and field distributions can be obtained by the matrix method.

We are looking for guided waves propagating in the positive z direction. Two important periodic multichannel waveguides will be considered in the following.

A. Symmetric type

Consider the simplest kind of symmetric PMDW with the index of refraction given by

$$n(x,z) = \begin{cases} n_2, & m\Lambda \le x \le m\Lambda + b \\ & (m = 0, 1, 2, \ldots, N-1), \\ n_1, & \text{otherwise}, \end{cases} \tag{40}$$

with

$$n_1 < n_2 .$$

The geometry of the waveguide is sketched in Fig. 9.

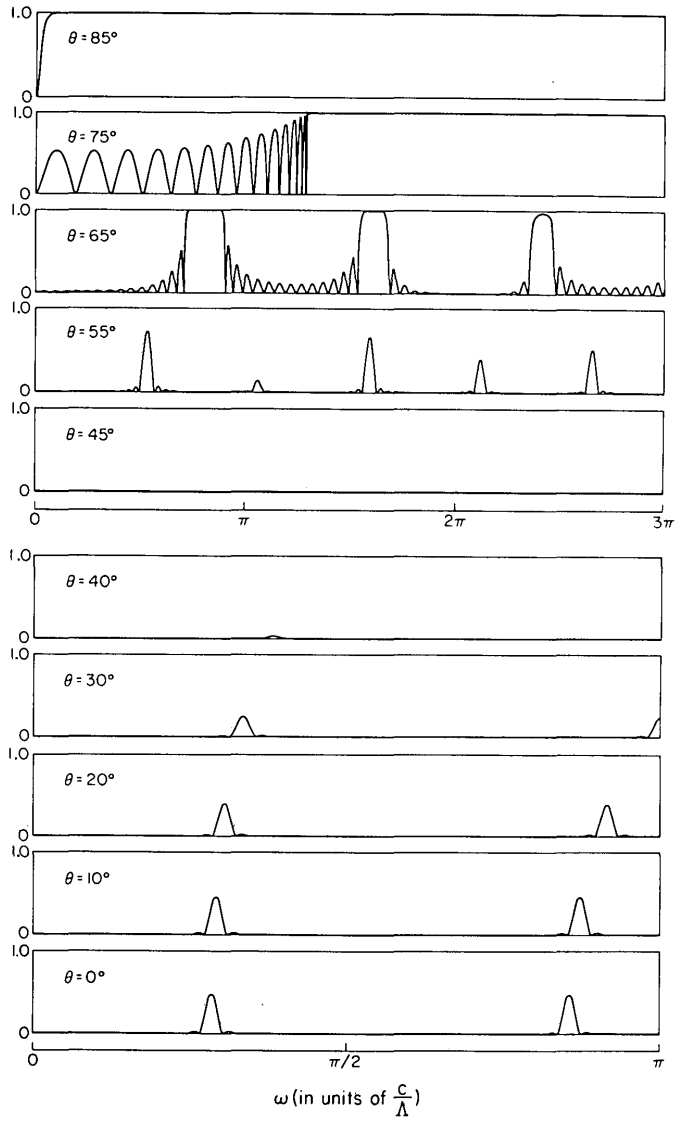

FIG. 8. TM waves reflectivity spectrum of a 15-period Bragg reflector at various angles of incidence.

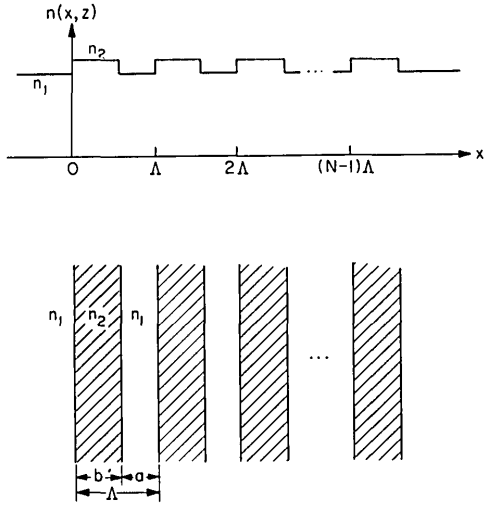

FIG. 9. Section view of a typical N-channel symmetric waveguide.

We will limit our analysis to TE waves only. It was shown in Sec. II that the translation matrix T which relates the field vector in one period to that of the next one is given by

$$T=\begin{pmatrix} A & B \\ C & D \end{pmatrix}, \tag{42}$$

where, after defining $-ik_{1x}=q$, $k_{2x}=p$, we get

$$\begin{aligned} A &= e^{qa}\left[\cos pb-\tfrac{1}{2}(p/q-q/p)\sin pb\right], \\ B &= e^{-qa}\left[-\tfrac{1}{2}(p/q+q/p)\sin pb\right], \\ C &= e^{qa}\left[\tfrac{1}{2}(p/q+q/p)\sin pb\right], \\ D &= e^{-qa}\left[\cos pb+\tfrac{1}{2}(p/q-q/p)\sin pb\right], \end{aligned} \tag{43}$$

with

$$\begin{aligned} q &= \{\beta^2-[(\omega/c)n_1]^2\}^{1/2}=-ik_{1x}, \\ p &= \{[(\omega/c)n_2]^2-\beta^2\}^{1/2}=k_{2x}. \end{aligned} \tag{44}$$

Since we are interested in guided waves only, the fields must be evanescent in the n_1 layer. We set $a_0=b_N=0$ in (30); since only outward radiating waves can be presented in a waveguide, the mode dispersion relation is

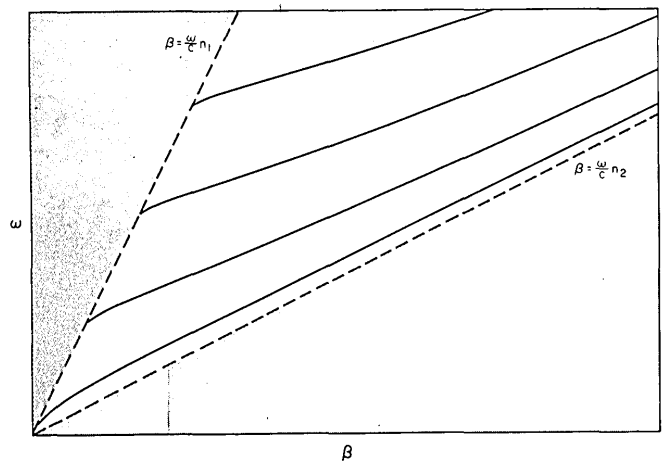

FIG. 10. Dispersion curves for the confined modes of a typical single channel waveguide ($N=1$).

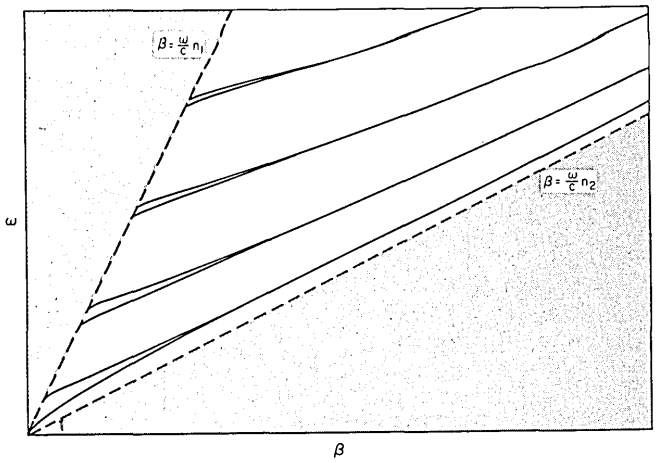

FIG. 11. Dispersion curves for the confined modes of a typical two-channel waveguide ($N=2$). Note the splitting in comparison with Fig. 10.

immediately obtained from (30) and (31),

$$A\left(\frac{\sin NK\Lambda}{\sin K\Lambda}\right)-\left(\frac{\sin(N-1)K\Lambda}{\sin K\Lambda}\right)=0. \tag{45}$$

If the left-hand side of (45) is plotted using (27) as a function of β for a given frequency ω, the zeros are the mode propagation constants (β's). It can be shown mathematically that there are exactly N zeros in each allowed band where $K\Lambda$ varies from $m\pi$ to $(m+1)\pi$ and none elsewhere. Physically the waveguide can be considered as a system of N interacting slab waveguides. The N modes are simply due to the splitting of an N-fold degenerate band as the separations between the N identical slab waveguides are reduced from infinity. Each confined mode of the single slab waveguide thus gives rise to a band with N nondegenerate modes. The dispersion relation (ω vs β) is shown in Figs. 10 and 11.

B. Asymmetric type

Consider a simple asymmetric N-channel waveguide with the following index of refraction:

$$n(x,z)=\begin{cases} n_a, & x<0, \\ n_2, & m\Lambda\le x<m\Lambda+b \\ & \quad (m=0,1,2,\ldots,N-1), \\ n_1, & \text{otherwise}. \end{cases} \tag{46}$$

The grand matrix which relates

$$\begin{pmatrix} a_0 \\ b_0 \end{pmatrix} \text{ to } \begin{pmatrix} a_N \\ b_N \end{pmatrix}$$

in this case is easily obtained from the continuity condition (6) and is given by

$$M=\begin{pmatrix} \frac{1}{2}(1+q/q_a) & \frac{1}{2}(1-q/q_a) \\ \frac{1}{2}(1-q/q_a) & \frac{1}{2}(1+q/q_a) \end{pmatrix}\begin{pmatrix} A & B \\ C & D \end{pmatrix}^N, \tag{47}$$

where

$$q_a=\{\beta^2-[(\omega/c)n_a]^2\}^{1/2}.$$

The first matrix of the matrix product in (47) accounts for the replacement of n_1 by n_a. Similarly, the mode dispersion relation is given by

$$\left(A+\frac{q_a-q}{q_a+q}C\right)\frac{\sin NK\Lambda}{\sin K\Lambda}-\frac{\sin(N-1)K\Lambda}{\sin K\Lambda}=0\ . \tag{48}$$

The eigenvalues β are determined as in the symmetric case (45). Equation (48) can be reduced to Eq. (45), which is the mode condition for a symmetric N-channel waveguide by setting $n_a=n_1$.

Associated with each β of a confined mode at a given frequency, there is a corresponding Bloch K vector given by (27). Instead of having all eigenvalues (β's) in the allowed band, an asymmetric periodic N-channel waveguide can have some eigenvalues (β's) with corresponding complex K and thus be in the "forbidden" band. These modes can be traced in terms of perturbation theory to the unperturbed modes of the surface channels in terms of perturbation theory. The characteristics of those modes are the localization of energy near the surface. Eigenvalues (β's) of the confined modes as a function of the separation between the neighboring channels are shown in Figs. 12 and 13 for two typical waveguiding structures. The band edges of the infinite periodic medium are also shown in the same figures. For small separation, all the modes have their eigenvalues in the allowed bands. There are exactly N β levels in a complete band. At infinite separation the β levels consist of an $(N-1)$-fold degenerate state and one nondegenerate state. The $(N-1)$-fold degenerate state will split into a band of $N-1$ levels when the separation is finite. *Those $N-1$ levels are always in the allowed band regardless of separation. The crossing between the nondegenerate state and the band edge happens at some critical separation a_c.* The surface modes only exist when the separation is larger than a_c. The properties of surface mode will be discussed more thoroughly in Sec. VII.

The transverse field distributions for a few typical periodic multichannel asymmetric dielectric waveguides are shown in Figs. 14 and 15 with N equal to 2 and 5, respectively. Only the confined modes in the first allowed band which corresponds to the lowest-order modes of the uncoupled individual channel waveguide are shown. As we know, there are exactly N modes in each complete group. The modes will be designated as TE_{mn} and TM_{mn} with n as the band index ($n=0,1,2,\ldots$) and m as the mode index ($m=0,1,2,\ldots,N-1$). There are exactly $m+nN$ zero crossings in the transverse field distribution for the mnth mode with n zero crossings in each guiding channel and m zero crossings in the $N-1$ separation layers. The field can have at most one zero crossing in each separation layer where the wave is evanescent.

The field distribution depends strongly on the index of refraction of the superstrate n_a when n_a is near n_1. The variation for the fundamental mode is shown in Figs. 16 and 17 for $N=2,5$ respectively. There is a drastic change of the field distribution for the surface channel when n_a is varied slightly from n_1. This phenomenon will be very useful in branching waveguides if a superstrate material with electro-optical effect can be found so that n_a can be tuned slightly around n_1 by applying a dc field:

$$n_a=n_a(E^{dc}=0)+\alpha E^{dc}\ , \tag{49}$$

with

$$n_a(E^{dc}=0)=n_1\ . \tag{50}$$

This drastic change of the field distribution due to slight variation of n_a can be used in electro-optical modulation.[18]

In the above analysis we assumed that the refractive index of the substrate $n_s=n_1$ for the simplicity of calculation. This is the reason why only one surface mode is found. In general, if $n_1\neq n_s<n_2$, two surface modes will exist. This is similar to the surface states in a crystal where the number of surface states is equal to the number of surface atoms. Here the number of surface modes is equal to the number of surface channels.

It has been shown in the above analysis that there are exactly N modes in each band. However, not all the modes need be confined. A confined mode must have its propagation constant β satisfy

$$\beta_{min}<\beta<\beta_{max}\ , \tag{51}$$

with

$$\beta_{max}=(\omega/c)\,n_2\ , \tag{52}$$

$$\beta_{min}=\max\left(\frac{\omega}{c}n_a,\ \frac{\omega}{c}n_s\right), \tag{53}$$

so that the wave is propagating in the guiding channels and evanescent in the substrate and cladding regions. For large enough separation between channels the whole band of β levels will fall between β_{max} and β_{min} so that all the N modes are confined. As the guiding channels are brought closer together, the β levels "repel" each other. As a result some of the modes will find their β value expelled from the confined region in β space. Those modes are transformed into radiation modes ($\beta<\beta_{min}$). The transition is shown in Figs. 12 and 13.

VI. BRAGG REFLECTION WAVEGUIDES

Optical dielectric waveguides with a slab configuration are capable of supporting lossless confined modes provided the index of refraction of the inner layer exceeds the indices of the two bounding media. This condition is necessary to obtain an imaginary transverse propagation constant which corresponds to an evanescent decay of the mode field in the bounding media.

There are many practical situations where it is desirable or necessary to guide power in a layer with a lower index than that in the two bounding media. A prime example of such a case is the waveguide laser in which the inner layer is air. This situation leads to lossy (leaky) modes whose loss constant increases as the third power of the reciprocal thickness of the inner layer.

In what follows we will show that, in principle, lossless propagation is possible in a low-index slab pro-

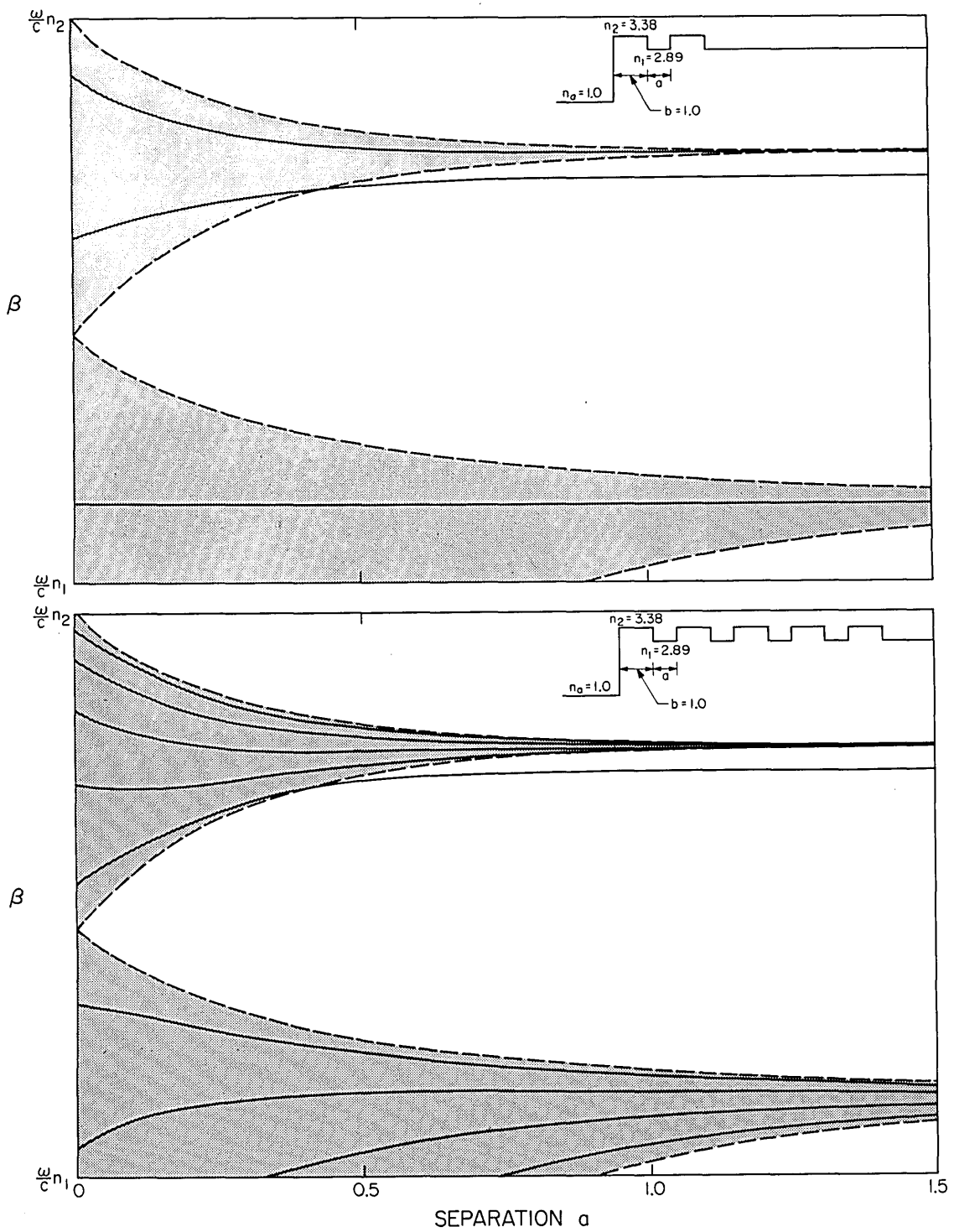

FIG. 12. β vs separation for two asymmetric multichannel waveguides with $N=2$ (upper diagram) and $N=5$ (lower diagram) at $\omega=\frac{3}{4}\pi c/a$. The dark zones are the allowed bands. Dashed curves are the band edges. The inset shows the refractive index profile.

vided the bounding media, with indices of refraction *larger* than that of the inner slab, are periodic. The model analyzed below assumes stratified periodic media. The use of stratified media in dielectric waveguiding has been proposed by Ash[19] who, however, did not consider the case of confined propagation in low index materials.

Referring to Fig. 18 we consider the case where $n_a < n_g < n_1, n_2$. In the case of TE modes the only field components are E_y, H_x, and H_z. Each of these components, say E_y, satisfies the wave equation

$$\frac{\partial^2 E_y}{\partial z^2} + \frac{\partial^2 E_y}{\partial x^2} + \frac{\omega^2}{c^2} n^2(x) E_y = 0 \,. \tag{54}$$

If we take $E_y(x, y, z) = E(x)\, e^{i\beta z}$ the wave equation becomes

$$\frac{\partial^2 E(x)}{\partial x^2} + \left(\frac{\omega^2}{c^2} n^2(x) - \beta^2\right) E(x) = 0 \,. \tag{55}$$

We take a solution in the form

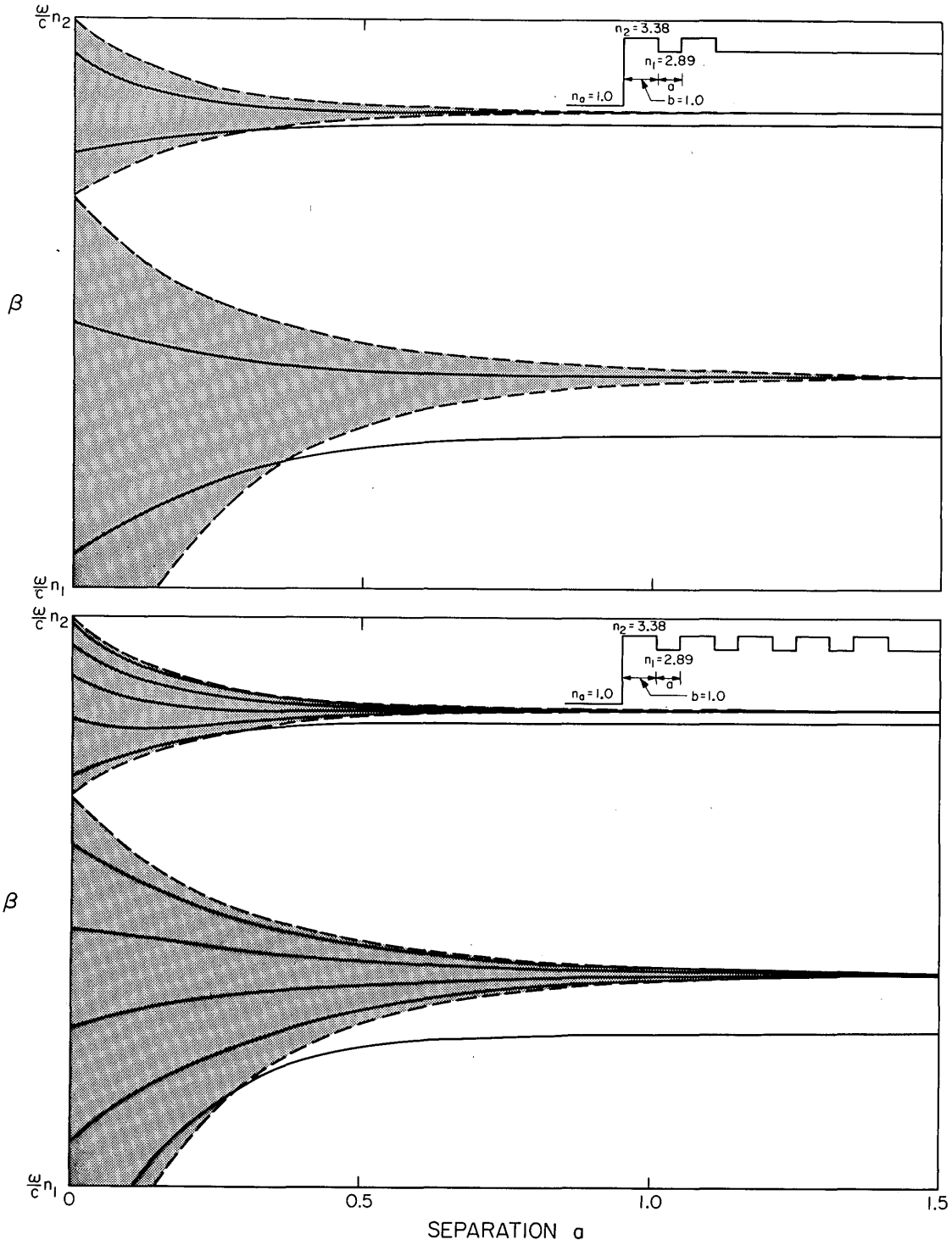

FIG. 13. β vs separation for two asymmetric multichannel waveguides with $N=2$ (upper diagram) and $N=5$ (lower diagram) at $\omega=\pi c/a$. The dark zones are the allowed bands. Dashed curves are the band edges. The inset shows the refractive index profile.

$$E(x)=\begin{cases}\text{(i) } e^{q_a(x+t)}, & x<-t,\\ \text{(ii) } c_1\cos(k_g x)+c_2\sin(k_g x), & -t\le x<0,\\ \text{(iii) } E_K(x)\,e^{iKx}, & 0\le x,\end{cases} \tag{56}$$

where

$$q_a=\left[\beta^2-\left(\frac{\omega}{c}n_a\right)^2\right]^{1/2},\quad k_g=\left[\left(\frac{\omega}{c}n_g\right)^2-\beta^2\right]^{1/2}. \tag{57}$$

The assumed solution in regions (i) and (ii) is identical to that of conventional slab dielectric waveguides.[20] The new feature in this case is the form of the wave $E_K(x)\,e^{iKx}$ in the stratified periodic medium (iii) where $E_K(x)\,e^{iKx}$ is given by (28).

It is important to note that the sign in front of the square root in (25) has to be the same as that of $\frac{1}{2}(A+D)$. This ensures that the Bloch wave is evanescent in the positive x direction.

To obtain the solution for the mode of the waveguide of Fig. 18 we match the fields and their x derivatives at $x=-t$. The result, using (26), (28), and (56), is the

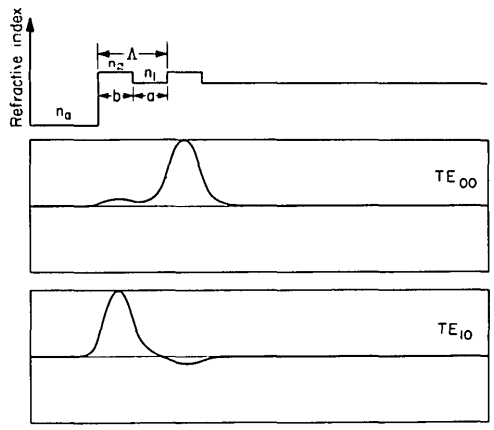

Transverse field distribution

FIG. 14. Transverse field distribution for the confined modes in the first band of a two-channel waveguide.

dispersion relation

$$k_g\left(\frac{q_a\cos k_g t - k_g \sin k_g t}{q_a \sin k_g t + k_g \cos k_g t}\right) = -ik_{1x}\frac{e^{-iK\Lambda} - A - B}{e^{-iK\Lambda} - A + B}. \qquad (58)$$

The left-hand side of (58) contains only parameters of the guiding (n_g) and substrate (n_a) layers while the right-hand side depends only on parameters of the periodic medium. For confined propagation β, q_a, and k_g are real so that the left-hand side of (58) is a real number. The right-hand side is real *only* when the propagating conditions in the periodic medium fall *within* one of the forbidden gaps, i.e., when $[\frac{1}{2}(A+D)]^2 > 1$. It follows that *confined lossless* modes of the composite waveguide (Fig. 18) exist. Operationally we may solve

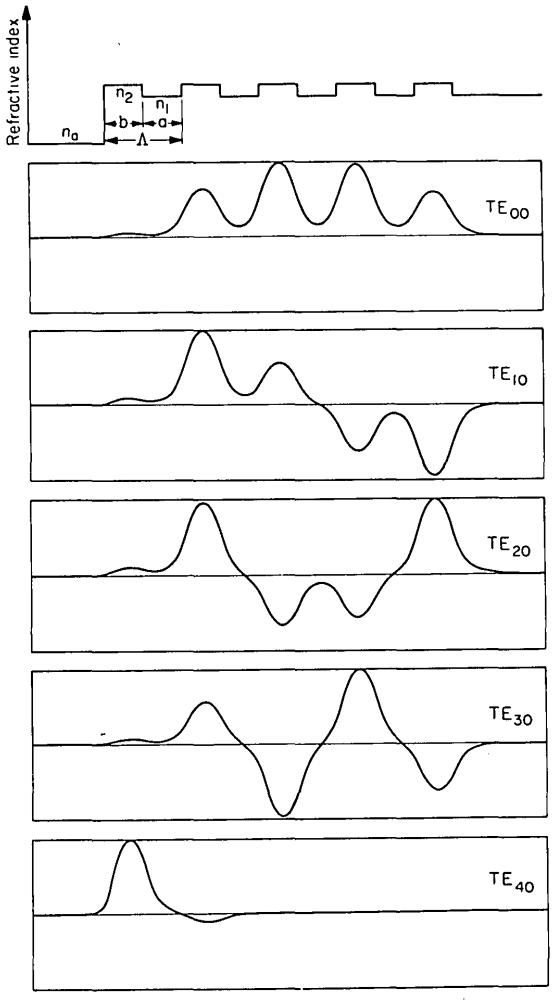

Transverse field distribution

FIG. 15. Transverse field distribution for the confined modes in the first band of a five-channel waveguide.

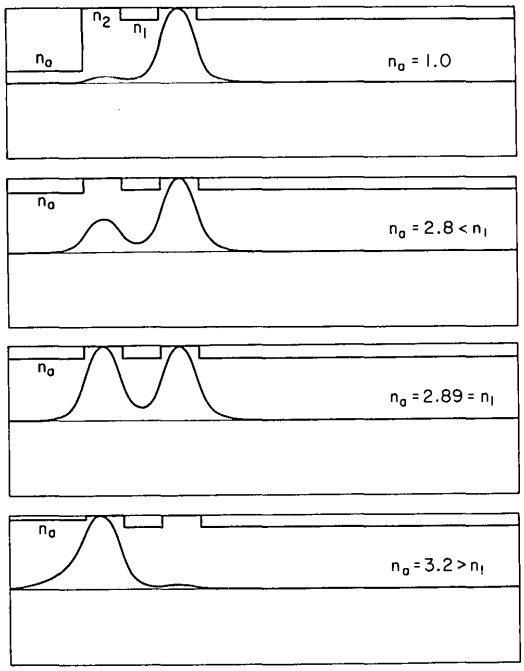

Transverse field distribution

FIG. 16. Transverse field distribution for the TE_{00} mode of a two-channel waveguide at various n_a's.

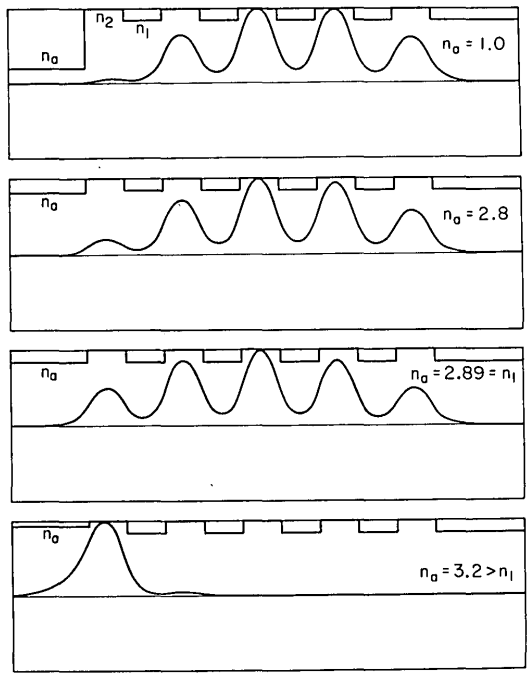

Transverse field distribution

FIG. 17. Transverse field distribution for the TE_{00} mode of a five-channel waveguide at various n_a's.

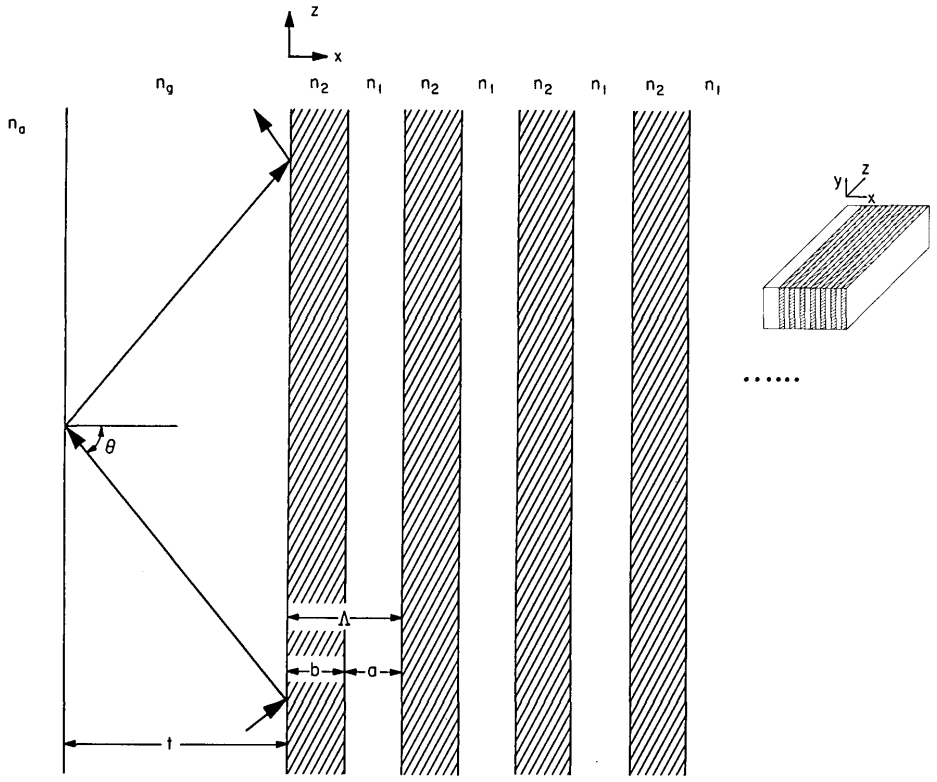

FIG. 18. Bragg reflection (slab) waveguide ($\partial/\partial y = 0$).

for the eigenmode by starting with some value of $\beta < (\omega/c)n_g$. This (for a given ω) determines k_g, q_a, k_{1x}, and k_{2x}. If the resulting values of A and D correspond to a forbidden gap $\{[\frac{1}{2}(A+D)]^2 > 1\}$, then the right-hand side of (58) is a (fixed) real number. We then proceed to adjust the thickness of the guiding layer t until an equality results. A simple physical description of the mathematical procedure just outlined is as follows: For *confined* and *lossless* mode propagation complete reflection must take place at the interface (see Fig. 18) between the guiding layer and the layered medium. This indeed occurs only when the zig-zagging wave is incident on the interface under conditions corresponding to that of a forbidden gap. All that remains to ensure a propagating mode is to choose the thickness t so that the transverse round-trip phase delay is some multiple of 2π.[21]

A calculated distribution of such a waveguide is shown in Fig. 19. Note that in the periodic (layered) medium the field corresponds to a periodic pattern under an evanescent envelope $e^{-K_1 x}$ as appropriate to a Bloch wave in a forbidden gap.

Also important is the fact that the evanescent decay is nearly complete in several periods so that practical structures with, say, ten unit cells are a good approximation to the semi-infinite layered medium assumed in the analysis.

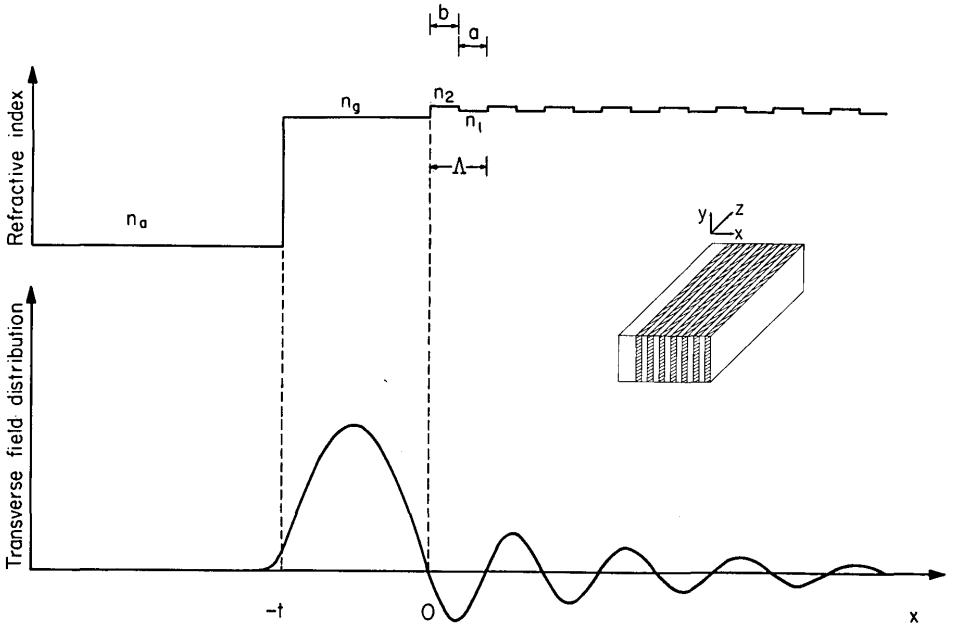

FIG. 19. Transverse field distribution of the fundamental modes of a typical Bragg reflection (slab) waveguide.

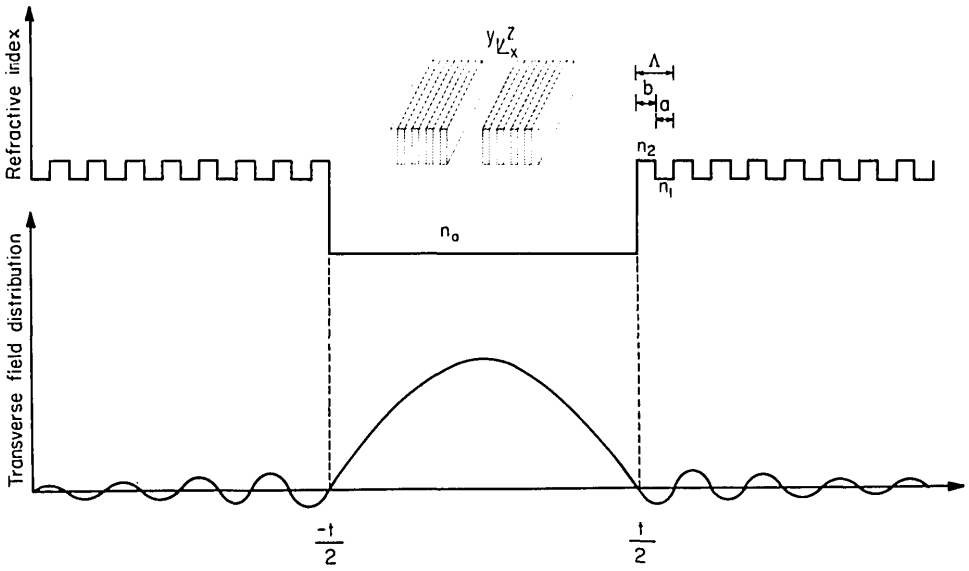

FIG. 20. Transverse field distribution of the fundamental mode of a typical Bragg reflection waveguide with air as the guiding channel.

A symmetric waveguide composed of a low-index slab, say air, separating two semi-infinite periodic media is of course also possible. Such a waveguide can be constructed by replacing the structure to the left of plane a (where $dE/dx = 0$) the structure to the right. The field distribution is then even symmetric about plane a. The result of such a procedure is shown in Fig. 20. Such a structure can be used as the waveguide for gaseous lasers.

Mathematically, the mode conditions for the TE modes of the symmetric Bragg waveguide can easily be shown to be

$$-ik_{1x}\left(\frac{e^{-iK\Lambda}-A-B}{e^{-iK\Lambda}-A+B}\right) = \begin{cases} -k_a \tan(\tfrac{1}{2}k_a t)\,, \\ \quad \text{even TE modes}\,, \\ k_a \cot(\tfrac{1}{2}k_a t)\,, \\ \quad \text{odd TE modes}\,, \end{cases} \tag{59}$$

where

$$k_a = \{[(\omega/c)n_a]^2 - \beta^2\}^{1/2}\,. \tag{60}$$

The Bragg waveguides described above should display strong discrimination against higher-order transverse modes, i.e., modes with a larger number of nodes in the central guiding region. This is due to the fact that the existence of a given mode requires, as discussed above, the simultaneous fulfillment of the transverse resonance condition within the guiding layer and the Bragg condition in the layered media. If the waveguide is designed so that these conditions are satisfied for a given transverse mode, they will not be satisfied by other transverse modes, except accidentally. We can show that if the waveguide is designed for the fundamental transverse mode ($s = 0$) then in order that the sth mode exist as well, the condition

$$\Lambda^2/t^2 = l/s\,, \quad l = 1, 2, 3, \ldots \tag{61}$$

need very nearly be satisfied. In Eq. (61) it was assumed that $(n_1 - n_2)/n_1 \ll 1$.

VII. ELECTROMAGNETIC SURFACE WAVES

It is the purpose of this section to investigate the electromagnetic surface waves guided by the boundary of a semi-infinite periodic multilayer dielectric medium. The surface wave, by definition, is a wave bounded by the interface between two semi-infinite systems. For example, the ripple phenomenon in water is a surface wave guided by the interface between air and water. Another interesting kind of surface wave is the electronic surface state which has been extensively studied in solid-state physics. The existence of localized modes ("surface states") near the interfaces of a layered medium and a homogeneous one was suggested by Kossel.[22] An approximate solution in the limit of loose binding was given by Arnaud and Saleh.[23] In this paper, the band theory of the periodic dielectric medium is employed to study the surface wave with an eigenvalue in the "forbidden" band.

The existence of a surface state can be explained as follows: In Sec. III we have shown that, at a given frequency, there are regions of β, for which K is complex and $K = m\pi/\Lambda \pm iK_i$. For an infinite periodic medium the exponential intensity variation cannot exist, and we refer to these regions as "forbidden." If the periodic medium is semi-infinite the exponentially damped solution is a legitimate solution near the interface and the field envelope decays as $e^{-K_i x}$, where x is the distance from the interface.

The existence of surface states can also be argued using perturbation theory. According to perturbation theory, the periodic multilayer dielectric medium which consists of alternating layers of different indices of refraction can be considered as a system of interacting waveguides. These waveguides are identical to each other except for the one near the surface. The interaction strength between the waveguides depends on the separation between the neighboring waveguides due to overlap of the evanescent field distributions. When the separation is infinite, there is no interaction and the guides can be considered as independent of each other. The eigenvalues (β's) thus fall into two groups: One is

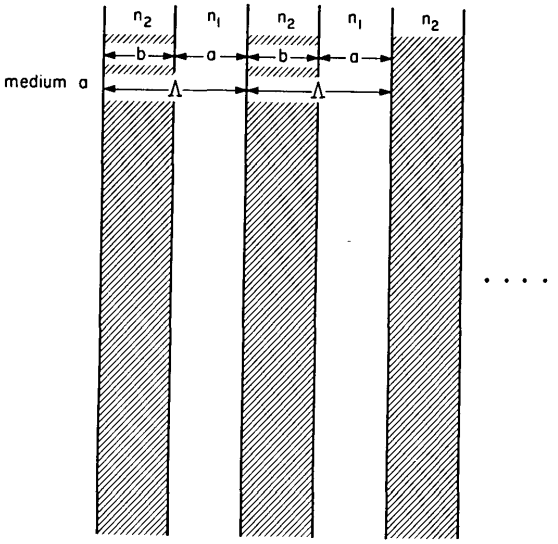

FIG. 21. Semi-infinite periodic stratified medium.

an infinitely degenerate state, the other is a nondegenerate state which corresponds to the extreme guide near the surface. As the waveguides are brought together, the interaction between the waveguides causes the eigenvalues to split. The splitting is shown in Figs. 12 and 13. As the eigenvalues split, the allowed energy band for the infinite structure is fully occupied by the levels originating in the infinitely degenerate level. As a result, the nondegenerate level corresponding to the waveguide near the surface will be expelled out of the allowed energy band. The only place where this state can be accommodated is in the forbidden gap. The field distribution for this state is localized near the surface because of the fact that the corresponding eigenvalue is in the "forbidden" band, i.e., $K = m\pi/\Lambda + iK_i$.

To investigate the properties of the surface modes consider a semi-infinite periodic multilayer dielectric medium consisting of alternating layers of different indices of refraction. The distribution of the indices of refraction is

$$n(x,z) = \begin{cases} n_a, & x \le 0 , \\ n_2, & m\Lambda \le x < m\Lambda + b , \\ n_1, & m\Lambda + b \le x < (m+1)\Lambda \\ & (m = 0,\ 1,\ 2,\ \ldots) . \end{cases} \tag{62}$$

The geometry of the structure is sketched in Fig. 21. We look for the possibility of waves propagating in the positive z direction. Since the structure is semi-infinite, we are only interested in the surface wave as far as guiding is concerned. For the sake of definiteness we consider the case of TE surface modes where the electric field is polarized in the y direction. The electric field distribution (TE) obeys the wave equation (54). We take the solution of (55) in the following form:

$$E(x) = \begin{cases} \alpha\, e^{q_a x}, & x \le 0 , \\ E_K(x)\, e^{iKx}, & x \ge 0 , \end{cases} \tag{63}$$

where q_a is given by

$$q_a = \{\beta^2 - [(\omega/c)n_a]^2\}^{1/2} , \tag{57}$$

and α is a constant.

In order to be a guided wave, the constant K in (63) must be complex so that the field decays as x goes to infinity. This is possible only when the propagating conditions (i.e., β) in the periodic medium correspond to a "forbidden" band. Another condition is that $E(x)$ and its x derivative be continuous at the interface with medium a. This gives us the condition for surface modes

$$q_a = q(e^{-iK\Lambda} - A - B)/(e^{-iK\Lambda} - A + B) . \tag{64}$$

Equation (64) can also be obtained directly from (58) by setting $t = 0$ and $k_{1x} = iq$.

The field distributions of some typical surface waves are shown in Figs. 22 and 23. It is evident that the energy is more or less concentrated in the first few periods of the semi-infinite periodic medium. It can

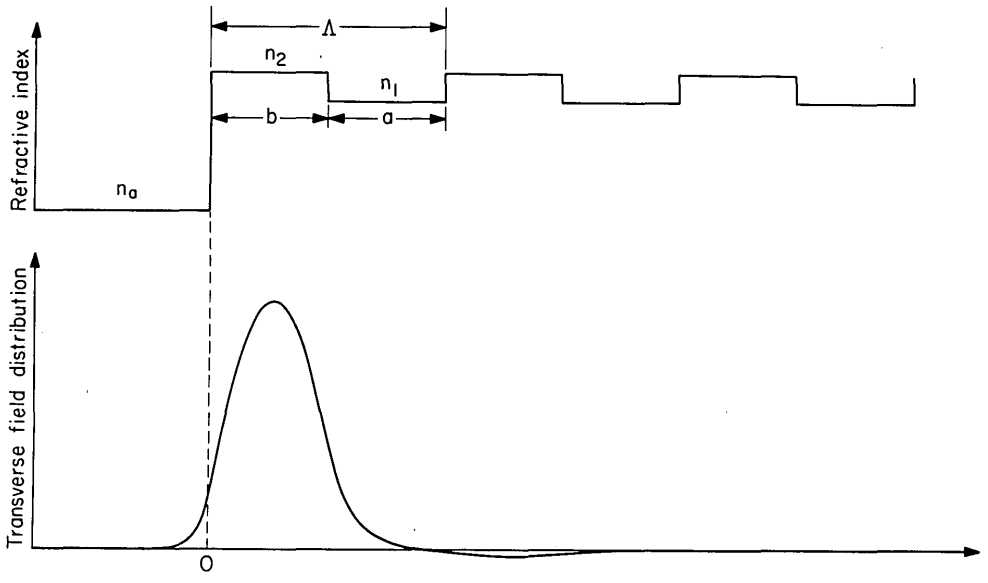

FIG. 22. Transverse field distribution for a typical fundamental surface mode guided by the surface of a semi-infinite periodic stratified medium.

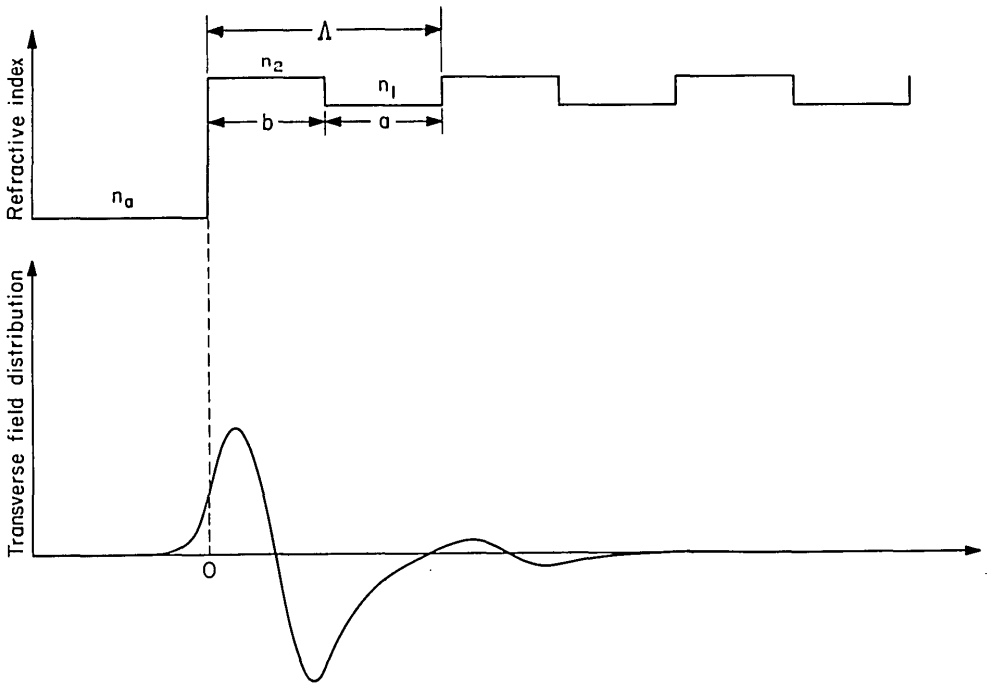

FIG. 23. Transverse field distribution for a typical higher-order surface mode guided by a semi-infinite peridic stratified medium.

easily be shown that

$$\frac{\text{energy in the first period}}{\text{energy in the whole semi-infinite periodic structure}} = (1 - e^{-2K_i\Lambda}) , \tag{65}$$

where K_i is the imaginary part of K. Generally speaking, the fundamental surface wave has the highest K_i and hence the highest degree of localization. The fundamental surface wave may happen to be in the zeroth or the first forbidden gap. It depends on the magnitude of the index of refraction n_a. For n_a less than n_1, which is a case of practical interest (n_a is the index of refraction of air), the fundamental surface wave has a Bloch wave vector in the first forbidden gap. This is due to the fact that when the waveguides are separated infinitely from each other the singlet state has an eigenvalue β lower than that of the infinitely degenerate state.

The field distribution in each period is similar to that of the distribution in the preceding period except that the amplitude is reduced by a factor of $(-1)^m e^{-K_i\Lambda}$, where m is the integer corresponding to the mth forbidden gap.

We have derived the mode condition for the surface wave by matching the boundary condition between an evanescent wave and a decaying Bloch wave. This electromagnetic surface wave is almost completely analogous to the surface state in solid-state physics. The existence of the surface mode in a semi-infinite structure is independent of the separation between waveguides, because the allowed band is always fully occupied. However, in a finite system, the allowed band is not fully occupied. As a result, the surface wave appears only when the separation is *large* enough so that one of the eigenvalues falls within the "forbidden" gap (see Figs. 12 and 13). This state of affairs is quite different from that of electronic surface states in crystals where, according to Shockley,[24] surface levels appear only when the interatomic distance becomes small enough so that the boundary curves of the allowed energy bands have crossed. The number of surface modes equal the number of modes that can be guided by the waveguide near the surface. This is very comprehensible in terms of perturbation theory.

The surface mode can still be guided when $n_2 < n_1$, however, the local extrema occur in the regions with index n_1 where the x dependence is sinusoidal. This is a general property of evanescent wave. The field distribution profile can bend at most once in the region where the wave is evanescent. The bending corresponds to a local minimum of the magnitude of field distribution. Because of the fact that $(1/E)(\partial^2 E/\partial x^2)$ is always positive, for $E > 0$, the field distribution profile is concave upward, while for $E < 0$, the field distribution profile is concave downward. This makes it impossible for $|E(x)|$ to possess a local maximum in the region where the wave is evanescent.

In the above analysis we assumed $(\omega/c)n_1 < \beta < (\omega/c)n_2$ so that the field is propagating (i.e., has a sinusoidal x profile) in the higher index medium while being evanescent in the lower index medium. However, this condition is not necessary. Surface waves exist also when $\beta < (\omega/c)n_{1,2}$. The analysis in this case is exactly the same as that above except that q has to be replaced by $-ik_{1x}$. The guiding, however, is not as tight as that of the former case, since the Bloch waves decay faster whenever there is a region where the wave is evanescent.

The surface wave does not exist, however, when $\beta > (\omega/c)n_{1,2}$ since in this case $(1/E)\partial^2 E/\partial x^2 > 0$ everywhere so that if the field is evanescent in the homogeneous medium a, it will increase without bound in the periodic medium and vice versa.

VIII. CONCLUSIONS

We have employed the concepts of Bloch waves and band structures to study periodically layered media. Analytic expressions for reflectivity, mode dispersion relations for Bragg waveguides and multichannel waveguides were derived.

Many aspects of the optics of periodic layered media are closely analogous to the physics of electrons in crystals. We have already shown the existence of band structures and surface states. It is clear that other phenomena in solid state physics have their analog in the optics of periodic layered media.

We have also obtained exact solutions for the dispersion ω vs K, or β vs K, of the medium. This should prove useful in phase matching[25] in nonlinear optical applications as well as in electro-optical modulation.

The general formalism developed in this paper will be applied in the accompanying paper to consider a number of specific problems.

APPENDIX A

Translation matrices of a general periodic layered medium with the index of refraction given by

$$n(x)=\begin{cases} n_1, & x_0<x<x_1\ , \\ n_2, & x_1<x<x_2\ , \\ \vdots & \\ n_M, & x_{M-1}<x<x_M\ , \end{cases} \tag{A1}$$

$$n(x+\Lambda)=n(x),\quad \Lambda=x_M-x_0\ . \tag{A2}$$

There are M layers in each period. The thickness of the mth layer is given by

$$t_m=x_m-x_{m-1}\ . \tag{A3}$$

The electric field distribution in the mth layer of the nth unit cell is given by

$$E(x)=a_n^{(m)}e^{ik_{mx}(x-n\Lambda)}+b_n^{(m)}e^{-ik_{mx}(x-n\Lambda)}\ . \tag{A4}$$

The translation matrix that relates the $m$the layers of two neighboring unit cells is designated as $T^{(m)}$,

$$\begin{pmatrix} a_{n-1}^{(m)}e^{ik_{mx}x_m} \\ b_{n-1}^{(m)}e^{-ik_{mx}x_m}\end{pmatrix}=T^{(m)}\begin{pmatrix} a_n^{(m)}e^{ik_{mx}x_m} \\ b_n^{(m)}e^{-ik_{mx}x_m}\end{pmatrix}\ . \tag{A5}$$

$T^{(m)}$ is derived by employing the continuity conditions:

$$T^{(m)}=\frac{1}{2^M}\prod_{\alpha=m+1}^{M+m}\begin{pmatrix}(1+C_\alpha)e^{-ik_{\alpha x}t_\alpha} & (1-C_\alpha)e^{ik_{\alpha x}t_\alpha} \\ (1-C_\alpha)e^{-ik_{\alpha x}t_\alpha} & (1+C_\alpha)e^{ik_{\alpha x}t_\alpha}\end{pmatrix}, \tag{A6}$$

where

$$C_\alpha=\begin{cases} k_{\alpha x}/k_{(\alpha-1)x}, & \text{TE waves}\ , \\ n_\alpha^2 k_{(\alpha-1)x}/n_{(\alpha-1)}^2 k_{\alpha x}, & \text{TM waves}\ . \end{cases} \tag{A7}$$

Note that

$$C_{M+\alpha}=C_\alpha,\quad t_{M+\alpha}=t_\alpha \tag{A8}$$

and

$$\prod_{\alpha=1}^{M}C_\alpha=1,\quad \sum_{\alpha=1}^{M}t_\alpha=\Lambda\ . \tag{A9}$$

The translation operator $T^{(m)}$ is formed by a product of M matrices. A cyclic permutation of the order of multiplication yields $T^{(m+1)}$. The translation operators for different m values are different but have the same eigenvalues.

If $\mu\neq$ constant, then

$$C_\alpha=\begin{cases} k_{\alpha x}\mu_{\alpha-1}/k_{(\alpha-1)x}\mu_\alpha, & \text{TE waves}\ , \\ n_\alpha^2 k_{(\alpha-1)x}\mu_{\alpha-1}/n_{\alpha-1}^2 k_{\alpha x}\mu_\alpha, & \text{TM waves}. \end{cases} \tag{A10}$$

APPENDIX B: DERIVATION OF CHEBYSHEV IDENTITY

The Nth power of a unimodular matrix can be simplified as shown in the following equation:

$$\begin{pmatrix} A & B \\ C & D\end{pmatrix}^N=\begin{pmatrix} AU_{N-1}-U_{N-2} & BU_{N-1} \\ CU_{N-1} & DU_{N-1}-U_{N-2}\end{pmatrix}, \tag{B1}$$

where

$$U_N=\sin(N+1)K\Lambda/\sin K\Lambda\ , \tag{B2}$$

with

$$K\Lambda=\cos^{-1}[\tfrac{1}{2}(A+D)] \tag{B3}$$

Proof: Let $V_\pm$ be the normalized eigenvectors of the $ABCD$ matrix with eigenvalues $e^{\pm iK\Lambda}$, respectively.

$$\begin{pmatrix} A & B \\ C & D\end{pmatrix}V_\pm=e^{\pm iK\Lambda}V_\pm\ . \tag{B4}$$

It is evident that the two eigenvalues are inverse of each other because of the fact that the matrix in (B4) is unimodular. They are given by

$$e^{\pm iK\Lambda}=[\tfrac{1}{2}(A+D)]\pm\{[\tfrac{1}{2}(A+D)]^2-1\}^{1/2}\ , \tag{B5}$$

with the corresponding eigenvectors given by

$$V_\pm=\begin{pmatrix}\alpha_\pm \\ \beta_\pm\end{pmatrix} \tag{B6}$$

where

$$\alpha_\pm=\frac{B}{[B^2+(e^{\pm iK\Lambda}-A)^2]^{1/2}},\quad \beta_\pm=\frac{e^{\pm iK\Lambda}-A}{[B^2+(e^{\pm iK\Lambda}-A)^2]^{1/2}}\ . \tag{B7}$$

The Chebyshev identity (B1) can be derived by employing the following matrix equation:

$$\left\{M\begin{pmatrix} A & B \\ C & D\end{pmatrix}M^{-1}\right\}^N=M\begin{pmatrix} A & B \\ C & D\end{pmatrix}^N M^{-1}\ , \tag{B8}$$

which says that the Nth power of a transformed matrix is equal to the transform of the Nth power of the original matrix. If a matrix M can be found such that

$$M\begin{pmatrix} A & B \\ C & D \end{pmatrix} M^{-1} = \begin{pmatrix} e^{iK\Lambda} & 0 \\ 0 & e^{-iK\Lambda} \end{pmatrix}, \tag{B9}$$

then the Nth power of the $ABCD$ matrix is immediately given by

$$\begin{pmatrix} A & B \\ C & D \end{pmatrix}^N = M^{-1}\begin{pmatrix} e^{iNK\Lambda} & 0 \\ 0 & e^{-iNK\Lambda} \end{pmatrix} M . \tag{B10}$$

The matrix M which transforms the $ABCD$ matrix into a diagonal matrix can be constructed from the eigenvectors (B6) of the $ABCD$ matrix. M and its inverse M^{-1} are given by

$$M^{-1} = \frac{1}{(\alpha_+\beta_- - \alpha_-\beta_+)^{1/2}}\begin{pmatrix} \alpha_+ & \alpha_- \\ \beta_+ & \beta_- \end{pmatrix}, \tag{B11}$$

$$M = \frac{1}{(\alpha_+\beta_- - \alpha_-\beta_+)^{1/2}}\begin{pmatrix} \beta_- & -\alpha_- \\ -\beta_+ & \alpha_+ \end{pmatrix} . \tag{B12}$$

The two columns in (B11) are simply the eigenvectors of the $ABCD$ matrix. It can be easily seen by simple matrix multiplication that (B9) is true as long as M and M^{-1} are given by (B12) and (B11), respectively. The Chebyshev identity (B1) follows directly from (B10) by carrying out the matrix multiplication:

$$\begin{pmatrix} A & B \\ C & D \end{pmatrix}^N = \frac{1}{\alpha_+\beta_- - \alpha_-\beta_+}\begin{pmatrix} \alpha_+ & \alpha_- \\ \beta_+ & \beta_- \end{pmatrix} \times \begin{pmatrix} e^{iNK\Lambda} & 0 \\ 0 & e^{-iNK\Lambda} \end{pmatrix}\begin{pmatrix} \beta_- & -\alpha_- \\ -\beta_+ & \alpha_+ \end{pmatrix}$$

$$= \begin{pmatrix} \dfrac{A\sin NK\Lambda - \sin(N-1)K\Lambda}{\sin K\Lambda} & \dfrac{B\sin NK\Lambda}{\sin K\Lambda} \\ \dfrac{C\sin NK\Lambda}{\sin K\Lambda} & \dfrac{D\sin NK\Lambda - \sin(N-1)K\Lambda}{\sin K\Lambda} \end{pmatrix}. \tag{B14}$$

The last step is left to the reader.

*Research supported by the Office of Naval Research and the NSF.

[1]F. Abeles, Ann. Phys. (Paris) 5, 596 (1950); 5, 706 (1950).
[2]A. Ashkin and A. Yariv, Bell Labs. Tech. Memo MM-61-124-46 (13 November 1961) (unpublished).
[3]N. Bloembergen and A. J. Sievers, Appl. Phys. Lett. 17, 483 (1970).
[4]C. L. Tang and P. P. Bey, IEEE J. Quantum Electron. QE-9, 9 (1973).
[5]S. M. Rytov, Zh. Eksp. Teor. Fiz. 29, 605 (1955) [Sov. Phys.-JETP 2, 466 (1956)].
[6]J. P. van der Ziel, M. Illegems, and R. M. Mikulyak, Appl. Phys. Lett. 28, 735 (1976).
[7]A. Y. Cho and J. R. Arthur, *Progress in Solid State Chemistry*, Vol. 10 (Pergamon, New York, 1975), Part 3, pp. 157 157–191.
[8]A. Yariv, Appl. Phys. Lett. 25, 105 (1974).
[9]F. Bloch, Z. Phys. 52, 555 (1928).
[10]K. Aiki, M. Nakamura, J. Umeda, A. Yariv, A. Katzir, and H. W. Yen, Appl. Phys. Lett. 27, 145 (1975).
[11]H. C. Casey, Jr., S. Somekh, and M. Ilegems, Appl. Phys. Lett. 27, 142 (1975).
[12]F. K. Reinhart, R. A. Logan, and C. V. Shank, Appl. Phys. Lett. 27, 45 (1975).
[13]A. Yariv, IEEE J. Quant. Electron. QE-9, 919 (1973).
[14]M. Born and E. Wolf, *Principles of Optics* (Macmillan, New York, 1964), p. 67.
[15]H. Yajima, Proceedings of the Symposium on Optical and Acoustical Micro-Electronics, New York, April 1974) (unpublished).
[16]L. B. Stotts, Opt. Commun. 17, 133 (1976).
[17]S. Somekh, E. Garmire, A. Yariv, H. Garvin, and R. Hunsperger, Appl. Phys. Lett. 22, 46 (1973).
[18]A. B. Buckman, J. Opt. Soc. Am. 66, 30 (1976).
[19]E. A. Ash, "Grating Surface Waveguides," presented at International Microwave Symposium, Newport Beach, Calif., May 1970 (unpublished).
[20]A. Yariv, *Quantum Electronics* (Wiley, New York, 1975).
[21]P. K. Tien, Appl. Opt. 10, 2395 (1971).
[22]D. Kossel, "Analogies between Thin-Film Optics and Electron-Band Theory of Solids," J. Opt. Soc. Am. 56, 1434 (1966).
[23]J. A. Arnaud and A. A. M. Saleh, Appl. Opt. 13, 2343 (1974).
[24]W. Shockley, Phys. Rev. 56, 317 (1939).
[25]J. P. van der Ziel and M. Ilegems, Appl. Phys. Lett. 28, 437 (1976).

Electromagnetic propagation in periodic stratified media. II. Birefringence, phase matching, and x-ray lasers*

Amnon Yariv and Pochi Yeh
California Institute of Technology, Pasadena, California 91125
(Received 8 November 1976)

The theory of electromagnetic Bloch waves in periodic stratified media is applied to the problems of birefringence and group velocity in these media. The relevance of periodic media to phase matching in nonlinear mixing experiments and to laser action in the x-ray region is discussed.

I. PHASE VELOCITY AND GROUP VELOCITY

We have derived in paper I[1] some of the important characteristics of Bloch waves propagating in a periodic stratified medium. An exact expression for the dispersion relation between K, β, and ω was derived. This dispersion relation can be represented by contours of constant frequency in the β-K plane as in Fig. 1.

It can be seen that these contours are more or less